Thin Solid Films xxx (2014) xxx–xxx

Contents lists available at ScienceDirect

Thin Solid Films

journal homepage: www.elsevier.com/locate/tsf

Photovoltaic performance of a $Cd_{1-x}Mg_xTe$/CdS top-cell structure

Omar S. Martinez [a,b], E. Regalado-Pérez [a], N.R. Mathews [a], Erik R. Morales [c], David Reyes-Coronado [d], Geovanni Hernández Galvez [b], Xavier Mathew [a,*]

[a] Instituto de Energías Renovables, Universidad Nacional Autónoma de México, Temixco, Morelos 62580, Mexico
[b] Centro del Cambio Global y la Sustentabilidad en el Sureste, Villahermosa, Tabasco 86080, Mexico
[c] División Académica de Ingeniería y Arquitectura, Universidad Juárez Autónoma de Tabasco, Cunduacán, Tabasco 86690, Mexico
[d] Unidad Académica Playa del Carmen, Universidad de Quintana Roo, Playa del Carmen, Quintana Roo 77710, Mexico

ARTICLE INFO

Available online xxxx

Keywords:
Cadmium magnesium telluride
Top-cell
Solar cells
Cadmium chloride vapor treatments

ABSTRACT

In this paper we report the progress in developing a wide band gap alloy material based on CdTe to use as the top-cell absorber in tandem solar cells. High photovoltaic performance for a $Cd_{1-x}Mg_xTe$/CdS top-cell was achieved by tuning the composition of the $Cd_{1-x}Mg_xTe$ film, and optimizing the device processing. We have carried out studies on the effect of vapor chloride treatment of the $Cd_{1-x}Mg_xTe$/CdS device and the thermal annealing of the Cu/Au contacts on the opto-electronic properties of the device. With improved contact processing and post deposition treatments, we were able to achieve 9.3% efficiency for a 1.6 eV band gap top-cell; $Cd_{1-x}Mg_xTe$/CdS on conductive glass substrate.

1. Introduction

CdTe is a potential II–VI group photovoltaic material that permits easy incorporation of elements such as Mg, Mn and Zn in the lattice, substituting the cation Cd [1–6]. The binary tellurides MgTe, MnTe and ZnTe have band gaps 3.5, 3.2 and 2.3 eV respectively [7–9] and can be easily alloyed with CdTe. Tolerance of CdTe in substituting Cd with these elements allows opening the band gap of CdTe in a wide range without altering significantly the structural parameters of CdTe. Among the above mentioned three elements, incorporation of Mg is more convenient since the band gap of CdTe can be significantly opened with a small quantity of Mg compared with other two elements [10]. In addition the lattice mismatch between CdTe and MgTe is less than 1% [3]. All these properties make $Cd_{1-x}Mg_xTe$ a promising top-cell material for applications in tandem solar cells.

We have reported the development of this ternary alloy by co-evaporation and a prototype $Cd_{1-x}Mg_xTe$/CdS device with an efficiency exceeding 4% [10]. Dhere et al. developed $Cd_{1-x}Mg_xTe$ alloys with band gaps ranging from 1.5 to 2.2 eV by co-evaporation and observed that the efficiency of $Cd_{1-x}Mg_xTe$/CdS device has an inverse dependence on the band gap of the alloy [1]. The highest reported efficiency for a $Cd_{1-x}Mg_xTe$/CdS device was 9.6% when the band gap of the alloy was 1.57 eV [11]; however, this band gap is in the lower limit to serve as an efficient top-cell absorber. In order to form part of a 25% efficient tandem cell, the band gap of the top-cell material should be more than 1.6 eV [12].

In this work we are discussing the development of $Cd_{1-x}Mg_xTe$ films with a band gap higher than 1.6 eV and report improved device efficiency due to the optimization of substrate temperature, $CdCl_2$ annealing process, and the Cu back contact diffusion. $Cd_{1-x}Mg_xTe$/CdS device with an efficiency of 9.3% was obtained, which is the highest reported efficiency of a $Cd_{1-x}Mg_xTe$/CdS device in which the band gap of the ternary alloy $Cd_{1-x}Mg_xTe$ is above 1.6 eV. This result shows that $Cd_{1-x}Mg_xTe$ with adequate band gap can be considered as a promising material to develop a top-cell for applications in tandem solar cells.

2. Experimental

The alloy films were deposited onto cleaned corning glass slides or CdS coated Pilkington NSG Tec™7 substrates by co-evaporation of Mg and CdTe at substrate temperatures in the range of 300–400 °C. The film stoichiometry was controlled by adjusting the deposition rate of CdTe and Mg independently. Band gaps of $Cd_{1-x}Mg_xTe$ films used in this study range from 1.6 to 1.7 eV. The X-ray diffraction (XRD) patterns of the films were recorded using a Rigaku X-ray diffractometer with Cu Kα ($\lambda = 1.54$ Å) radiation at a grazing angle of 0.5°. Band gaps of the materials were estimated from the transmittance spectra by plotting graphs of $(\alpha h\nu)^2$ against $h\nu$. The scanning electron microscopy (SEM) images of the films were recorded using a Hitachi S-5500 scanning microscope, operating at voltages 15 to 20 kV.

For device fabrication, CdS films of approximately 100 nm thicknesses were developed by chemical bath deposition [13] on well-cleaned Tec™7 substrates, and $Cd_{1-x}Mg_xTe$ film was deposited on top of CdS. All the films used in this work were of same thickness

* Corresponding author.
E-mail address: xm@ier.unam.mx (X. Mathew).

http://dx.doi.org/10.1016/j.tsf.2014.10.082
0040-6090/

Table 1
Optoelectronic properties of $Cd_{1-x}Mg_xTe$/CdS devices as a function of band gap (E_g)/Mg content (x) of the film. For a comparison: the efficiencies reported in literature for the $Cd_{1-x}Mg_xTe$ films with E_g values 1.57, 1.6 and 1.7 eV are 5.17, 4.87 and 4.08% respectively [1].

Film (given in the bracket are sample IDs)	E_g (eV)	Efficiency (%)	x
As-deposited (54D)	1.60	0.6	0.05
Annealed (54D)	1.60	4.1	0.05
Annealed (104)	1.64	3.5	0.06
Annealed (98)	1.70	2.8	0.08

(1.5 μm) and deposited under identical conditions. The $CdCl_2$ activation, contact formation, and the Cu back contact diffusion were performed on all devices in the same manner. The recrystallization and junction activation of $Cd_{1-x}Mg_xTe$/CdS heterostructure were achieved by annealing in the presence of $CdCl_2$ vapor under an ambient of Ar/O_2 in the temperature range 380–400 °C. The ambient was 50% Ar and 50% O_2 at a total pressure of 10 mbar. Prior to depositing the back contact, the $Cd_{1-x}Mg_xTe$ surface was cleaned by dipping in hot methanol, no acid etching was applied. The electrical contacts for the devices were obtained by sequentially depositing thin layers of Cu (3 nm) and Au (30 nm). The metal contacts were cured in a tube furnace at 150 °C for time durations between 0 and 40 min. The net carrier concentration (N_A–N_D) of the $Cd_{1-x}Mg_xTe$/CdS device at room temperature was estimated from capacitance–voltage (C–V) data collected using a Keithley 590 C–V analyzer at a frequency of 100 kHz. The current–voltage (J–V) data were collected under AM1.5, 100 mW/cm^2 illumination. The quantum efficiency (QE) data was normalized using a reference Si diode calibrated at NREL.

3. Results and discussion

3.1. Device characterization

Table 1 shows the optoelectronic properties of $Cd_{1-x}Mg_xTe$/CdS devices fabricated with $Cd_{1-x}Mg_xTe$ films of identical thickness, but band gap ranging from 1.6 to 1.7 eV. As expected, the efficiency of the device is higher when the band gap of the absorber is close to that of CdTe. The device efficiency has almost an inverse linear dependence on band gap. The observed decrease in efficiency is due to various reasons such as the distortion of unit cell due to incorporation of Mg, defects associated with incorporation of Mg, increase in band gap, and inefficient post-deposition thermal treatments. Similar tendency has been observed by Dhere et al. in the case of $Cd_{1-x}Mg_xTe$ films deposited by co-evaporation [1].

The QE of one of the $Cd_{1-x}Mg_xTe$/CdS solar cells along with that of a reference CdTe/CdS device is illustrated in Fig. 1. Two differences can be noticed in the QE of $Cd_{1-x}Mg_xTe$/CdS device with respect to the QE of CdTe/CdS: the blue shift in the long wavelength edge indicates a change in band gap due to the incorporation of Mg, and the relatively sharp edge at the CdS absorption region indicating little inter-diffusion of S and Te at the $Cd_{1-x}Mg_xTe$/CdS interface.

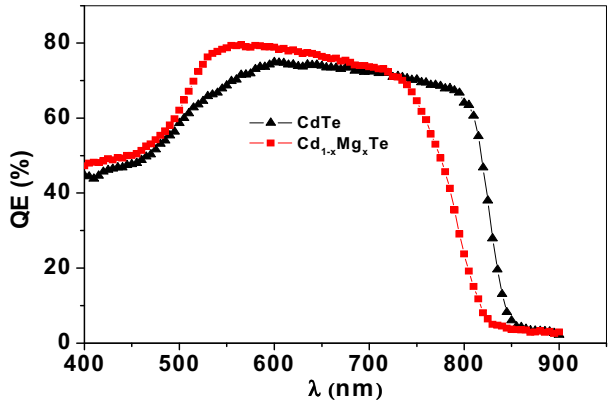

Fig. 1. Quantum efficiency spectra of $Cd_{1-x}Mg_xTe$/CdS and CdTe/CdS devices.

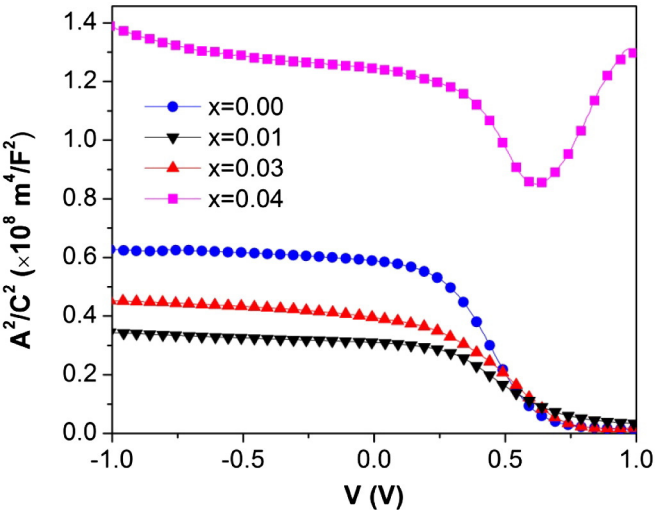

Fig. 2. Mott–Schottky plots for $Cd_{1-x}Mg_xTe$/CdS devices (x = 0.0, 0.01, 0.03 and 0.04).

The Mott–Schottky plots of the $Cd_{1-x}Mg_xTe$/CdS devices with x = 0.0, 0.01, 0.03 and 0.04 are presented in Fig. 2. Apparently, two different slopes exist in the plots: the calculated carrier densities deduced from $(A/C)^2$ vs. V at large reverse bias are associated with bulk doping, and at low forward bias correspond to the region near $Cd_{1-x}Mg_xTe$/CdS interface. For each device, the Mott–Schottky plot reveals that the capacitance practically does not vary with the inverse voltage, suggesting that the depletion region under reverse bias extends throughout the $Cd_{1-x}Mg_xTe$ layer. This is a typical behavior of a p-i-n type device where the highly resistive i-layer is totally depleted. An important observation in Fig. 2 is that at reverse bias, a device with 4% Mg exhibits a smaller effective capacitance than the other devices. In accordance with our J–V measurements (not shown), this is due to the presence of a rectifying back-contact in a device with 4% Mg, which leads to an additional capacitance in series and, consequently, to a decrease in the total capacitance. For devices with less than 3% Mg the rectifying effect is not observed in the J–V curves, so that the additional capacitance is negligible and the total cell capacitance is higher.

Fig. 3 displays the depth profiles of the net acceptor concentration in the $Cd_{1-x}Mg_xTe$ (x = 0.0, 0.01 and 0.03). Depth profiles display a

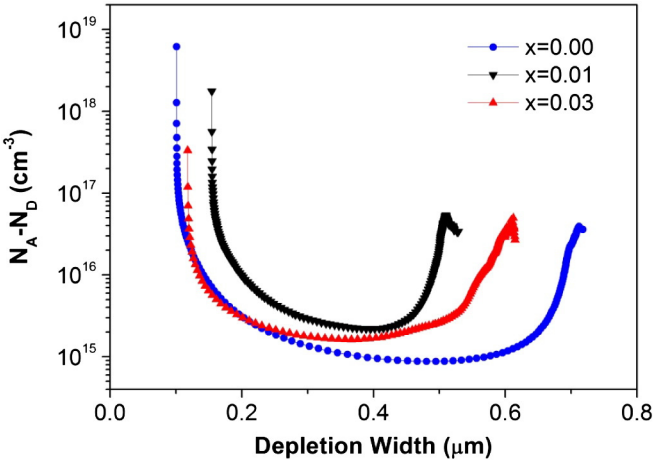

Fig. 3. Capacitance depth profiles for $Cd_{1-x}Mg_xTe$/CdS devices (x = 0.00, 0.01 and 0.03).

Please cite this article as: O.S. Martinez, et al., Photovoltaic performance of a $Cd_{1-x}Mg_xTe$/CdS top-cell structure, Thin Solid Films (2014), http://dx.doi.org/10.1016/j.tsf.2014.10.082

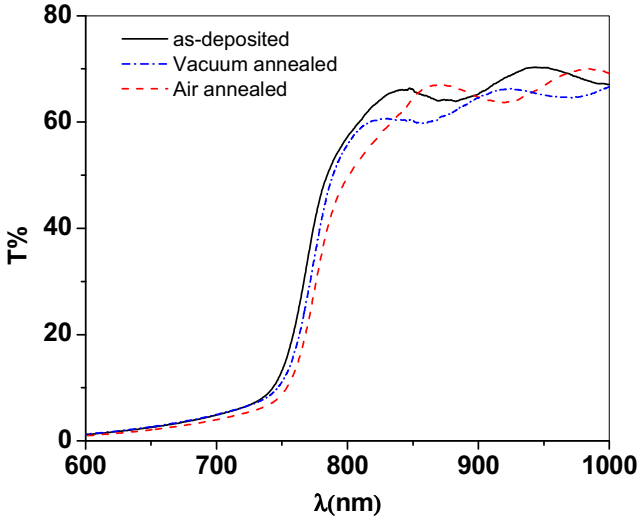

Fig. 4. Transmittance spectra of $Cd_{1-x}Mg_xTe$ Films: as-deposited, annealed with $CdCl_2$ in vacuum, and annealed with $CdCl_2$ in air.

characteristic U-shape, where the left branch corresponds to the forward bias condition while the right branch belongs to the reverse bias. The increase in the left branch may indicate actual charge distribution at the $Cd_{1-x}Mg_xTe$/CdS interface or non-uniform carrier density in its vicinity due to factors such as Te/S intermixing and/or the presence of Cu diffused from back contact, as reported by Li et al. [14] for CdTe solar cells. The bottom part of these profiles corresponds to the carrier density in the bulk of the absorber layer. A comparison of the profiles reveals that the incorporation of Mg in CdTe is beneficial as it increases the carrier density in the absorber. Also it can be observed that in all cases the carrier density increases by more than one order of magnitude in the back contact region, which can be mainly due to the presence of Cu related acceptors. This is expected since the back contact is Cu–Au.

3.2. Effect of post deposition treatments on the photovoltaic performance of the cell

It is known that in the case of CdTe, thermal annealing in the presence of $CdCl_2$ vapor and oxygen reduces the film resistivity and enhances the optoelectronic characteristics of devices [4,15]. Our studies revealed that in the case of $Cd_{1-x}Mg_xTe$ devices $CdCl_2$ treatment is necessary to obtain reasonably good efficiencies; however, the presence of oxygen in the treatment environment can cause stability issues owing to the affinity of Mg towards oxygen [3]. In order to isolate the issue of oxidation and to investigate only the effect of $CdCl_2$, we deposited a thin layer of $CdCl_2$ on the film surface and annealed in vacuum. Fig. 4 shows the transmittance spectra of a typical $Cd_{1-x}Mg_xTe$ film annealed in vacuum and in air (under atmospheric pressure and humidity of the laboratory), for comparison the spectrum of an as-deposited film is also shown. The vacuum and air annealing was at 400 °C, for 5 min. It can be seen that the film annealed in air shows a slight redshift for the absorption edge, indicating a decrease in band gap which is caused by the change in film stoichiometry. However, in our devices we do not expect a notable deterioration of the $Cd_{1-x}Mg_xTe$ film and band gap shrinking since the junction activation was performed under a much lower concentration of oxygen (Ar/O_2 ambient at 10 mbar pressure) compared to one atmospheric pressure of air as explained in Section 2. Further our previous studies showed that $Cd_{1-x}Mg_xTe$/CdS heterojunction is tolerant to short duration annealing in dry air [3].

Table 2
Device parameters of three typical $Cd_{1-x}Mg_xTe$/CdS solar cells in which the heterostructure was annealed in $CdCl_2$ vapor at 380, 390 and 400 °C for 5 min. The E_g of $Cd_{1-x}Mg_xTe$ was identical (1.6 eV) in all cases.

E_g (eV)	Anneal temp. (°C)	V_{oc} (mV)	J_{sc} (mA cm^{-2})	η (%)
1.6	380	566	10.3	3.8
	390	615	18.2	4.1
	400	696	13.7	5.8

The SEM images in Fig. 5 show the effect of $CdCl_2$ treatment on the recrystallization of $Cd_{1-x}Mg_xTe$ films; images A and B correspond respectively to films annealed without and with $CdCl_2$ at 400 °C. Effect of $CdCl_2$ in recrystallization is evident, however, not as prominent as that reported for CdTe films, which is due to the fact that the annealing duration was made shorter (5 min.) to prevent oxidation of Mg and subsequent decrease in film band gap. Average grain size was estimated in both cases and there is an increment of ≈50 nm for film recrystallized with $CdCl_2$, indicating less grain boundaries and a possible reduction in recombination losses. The effect of $CdCl_2$ re-crystallization temperature on the device parameters of $Cd_{1-x}Mg_xTe$/CdS solar cell is summarized in Table 2, band gap of the absorber was 1.6 eV. The Cu diffusion was performed at 150 °C for 40 min, which was established by the procedure discussed in Section 3.3. The significant influence of junction activation temperature on device parameters is clearly seen. The obtained parameters at 400 °C can be further improved if annealed for longer duration without causing film instability. However, a detailed

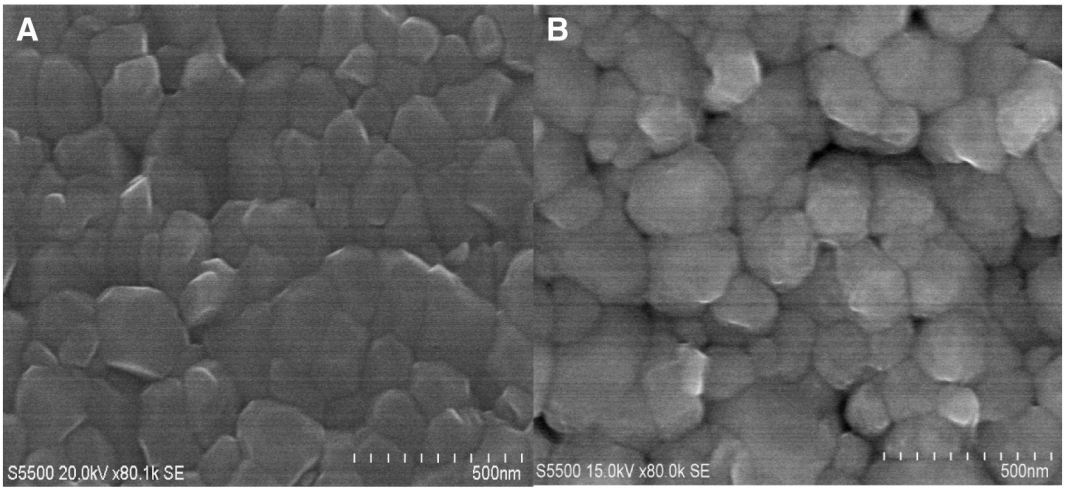

Fig. 5. SEM images of $Cd_{1-x}Mg_xTe$ films: A—annealed without $CdCl_2$, B—annealed in presence of $CdCl_2$. Annealing temperature was 400 °C for 5 min.

Please cite this article as: O.S. Martinez, et al., Photovoltaic performance of a $Cd_{1-x}Mg_xTe$/CdS top-cell structure, Thin Solid Films (2014), http://dx.doi.org/10.1016/j.tsf.2014.10.082

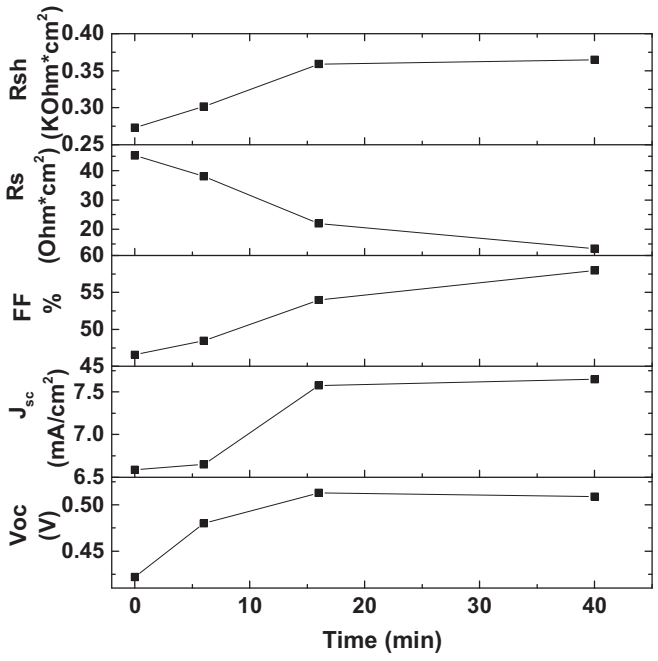

Fig. 6. Diffusion time of Cu contact vs. electrical parameters (V_{oc}, J_{sc}, FF, R_s and R_{sh}) of a typical $Cd_{1-x}Mg_xTe$/CdS device. Cu/Au = 3 nm/30 nm, temperature of diffusion 150 °C.

study is needed to optimize the junction activation temperature and film stoichiometry dependence.

3.3. Effect of Cu contact diffusion on the performance of the $Cd_{1-x}Mg_xTe$/CdS solar cells

We have investigated the effect of annealing of the Cu/Au back contact (Cu diffusion) on the electrical parameters of the $Cd_{1-x}Mg_xTe$/CdS device. The completed devices: Tec™7/CdS/$Cd_{1-x}Mg_xTe$/Cu–Au were annealed at 150 °C for a period of 0–40 min in order to permit Cu diffusion. The variation of open circuit voltage (V_{oc}), short circuit current density (J_{sc}), fill factor (FF), shunt resistance (R_{sh}) and series resistance (R_s) with Cu diffusion duration is shown in Fig. 6. The entire experiment was completed with the same device by measuring the current–voltage characteristics after each annealing step. As seen in the figure, the device parameters show a dependence on Cu diffusion time. The dependence is significant for the first 15 min, and for longer diffusion periods all the parameters except FF and R_s attain saturation. The dependence is noticeable in the case of R_s, which is reflected in the improved FF at longer annealing duration. The overall effect of Cu diffusion is the elimination of back-barrier resulting in a better ohmic contact. With a $Cd_{1-x}Mg_xTe$ absorber film having a 1.6 eV band gap, the efficiency of the best $Cd_{1-x}Mg_xTe$/CdS device obtained in this work was 9.3%. The device parameters are presented in Table 3.

4. Conclusions

Thin films of $Cd_{1-x}Mg_xTe$ with different compositions were developed by co-evaporation. Nearly optimum conditions for the $CdCl_2$ vapor treatments of the $Cd_{1-x}Mg_xTe$/CdS device and Cu diffusion of the back contact were established. It was observed that the practical $CdCl_2$ vapor treatment time window is short for $Cd_{1-x}Mg_xTe$ compared to that of CdTe, resulting in less recrystallization. With optimized processing conditions a prototype solar cell, based on the wide band gap alloy $Cd_{1-x}Mg_xTe$, with an efficiency of 9.3% was developed. The obtained efficiency for a 1.6 eV band gap material indicates that this material can be developed into a suitable top-cell absorber for tandem solar cells. Carrier concentration in the material was found to be higher at $Cd_{1-x}Mg_xTe$/CdS interface and at the back contact. The incorporation of Mg in CdTe is found to increase the carrier density in the film.

Table 3
Photovoltaic parameters of the best $Cd_{1-x}Mg_xTe$/CdS solar cell, which was $CdCl_2$ treated at 400 °C for 5 min. The back contact diffusion was performed at 150 °C for 40 min.

E_g (eV)	V_{oc} (mV)	J_{sc} (mA/cm²)	FF (%)	η (%)
1.6	727	23.3	55.2	9.3

Acknowledgments

This work at IER-UNAM was supported by the projects CeMIE-Sol 207450/P25, and SENER-CONACyT 117891. Authors acknowledge Gildardo Casarrubias Segura for his technical support in the laboratory and Maria L. Ramon Garcia for XRD analysis.

References

[1] R. Dhere, K. Ramanathan, J. Scharf, H. Moutinho, B. To, A. Duda, R. Noufi, Investigation of CdMgTe alloys for tandem solar cell applications, Proceedings Conference Record of the IEEE 4th World Conference on Photovoltaic Energy Conversion, 2006, p. 546 ((IEEE Cat. No. 06CH37747) IEEE).
[2] T. Shitaya, T. Ishida, H. Sato, Emission spectra of $Cd_{1-x}Mg_xTe$ light-emitting diodes, Appl. Phys. Lett. 21 (1972) 523.
[3] X. Mathew, J. Drayton, V. Parikh, N.R. Mathews, X. Liu, A.D. Compaan, Development of a semitransparent CdMgTe/CdS top cell for applications in tandem solar cell, Semicond. Sci. Technol. 24 (2009) 015012.
[4] O.S. Martinez, R.C. Palomera, J.S. Cruz, X. Mathew, Co-evaporated $Cd_{1-x}Mg_xTe$ thin films for applications in tandem solar cells, Phys. Status Solidi C 6 (2009) S214.
[5] X. Mathew, J. Drayton, V. Parikh, A.D. Compaan, Sputtered, $Cd_{1-x}Mg_xTe$ films for top cells in tandem devices, Proceedings Conference Record of the IEEE 4th World Conference on Photovoltaic Energy Conversion, 2006, p. 321 ((IEEE Cat. No. 06CH37747). IEEE).
[6] S. Hyun Leea, A. Guptaa, S. Wanga, A.D. Compaana, Brian E. McCandless, Sputtered $Cd_{1-x}Zn_xTe$ films for top junctions in tandem solar cells, Sol. Energy Mater. Sol. Cells 86 (2005) 551.
[7] J.M. Hartman, J. Cibert, F. Kany, H. Mariette, M. Charleux, P. Alleysson, R. Languer, G. Fuillet, CdTe/MgTe heterostructures: growth by atomic layer epitaxy and determination of MgTe parameters, J. Appl. Phys. 80 (1996) 6257.
[8] S.M. Durbin, J. Han, O. Sungki, M. Kobayashi, D.R. Menke, R.L. Gunshor, Q. Fu, N. Pelekanos, A.V. Nurmikko, D. Li, J. Gonsalves, N. Otsuka, Zinc-blende MnTe: epilayers and quantum well structures, Appl. Phys. Lett. 55 (20) (1989) 2087.
[9] T. Baron, K. Saminadayar, N. Magnea, Nitrogen doping of Te-based II–VI compounds during growth by molecular beam epitaxy, J. Appl. Phys. 83 (3) (1998) 1354.
[10] O.S. Martinez, R.C. Palomera, J.P. Enriquez, C.M. Alonso, X. Liu, N.R. Mathews, X. Mathew, A.D. Compaan, Development of Wide Band Gap $Cd_{1-x}Mg_xTe$/CdS Top Cells for Tandem Devices, Proceedings of 33rd IEEE PVSC, San Diego, CA, 2008 (5 pp).
[11] J.N. Duenow, R.G. Dhere, J. Li, W.K. Metzger, A. Duda, T.A. Gessert, Development of ZnTe contacts for $Cd_{1-x}Mg_xTe$ thin film solar cells for tandem, Applications Materials Research Society Symposium Proceedings, 1165, 2010, p. 405.
[12] Timothy J. Coutts, J. Scott Ward, David L. Young, Keith A. Emery, Timothy A. Gessert, Rommel Noufi, Critical issues in the design of polycrystalline, thin-film tandem solar cells, Prog. Photovolt. Res. Appl. 11 (2003) 359.
[13] Joel Pantoja Enr!ıquez, Xavier Mathew, Influence of the thickness on structural, optical and electrical properties of chemical bath deposited CdS thin films, Sol. Energy Mater. Sol. Cells 76 (2003) 313.
[14] J. Li, A. Halverson, O. Sulima, S. Bansal, J. Burst, T. Barnes, T. Gessert, D. Levi, Theoretical analysis of effects of deep level, back contact, and absorber thickness on capacitance–voltage profiling of CdTe thin-film solar cells, Sol. Energy Mater. Sol. Cells 100 (2012) 126.
[15] Ramesh Dhere, Kannan Ramanathan, John Scharf, David Young, Bobby To, Anna Duda, Helio Moutinho, Rommel Noufi, Fabrication and characterization of $Cd_{1-x}Mg_xTe$ thin films and their application in solar cells, Mater. Res. Soc. Proc. 1012 (2007) 37.